SPECTRO ELECTRO CHEMISTRY

Prof. B. Viswanathan
National Centre for Catalysis Research
IIT Madras, Chennai – 600 036

In situ Spectroelectrochemistry

The use of spectroscopic methods in different fields of electrochemistry is a landmark in modern electrochemical research. While spectroscopy follows the interaction of species like atoms, ions, molecules or extended systems with an electromagnetic radiation, electrochemistry deals with the charge transfer at a phase boundary of two condensed phases differing in its charge transport mechanism.[127] The interphase is the main subject of fundamental studies in electrochemistry where the transport and distribution of ions is dominating all processes and any chemical change in that interphase is the matter of study.[128] Therefore electrochemistry is focused on processes at interphases while spectroscopic methods are often dealing with bulk properties of different materials. The application of non-electrochemical methods in electrochemistry can be divided into two general cases:[129]

1) Ex situ methods (off-line): Realization of the (spectroscopic) measurement outside the electrochemical cell in an external device.

2) In situ methods (on-line): Realization of the measurement within an electrochemical experiment at the same electrode system.

Advantages of in situ measurements in electrochemical Studies

1. Direct access to kinetic data of electrode reactions.
2. Qualitative and quantitative information on the state of the interphase at electrochemical conditions.
3. Efficient set of experimental data (under variation of the different parameters) at high scan rates.
4. Fast repetition of experiments at different conditions including a computerized evaluation of the data.
5. Simultaneous acquisition of data from different methods in one single experiment.
6. Separation of the Faradaic and non-Faradaic part of an electrochemical reaction by a quantitative identification of the reaction products at the electrode.

Disadvantages of in situ electrochemical Studies

1. The low concentration of the reaction products at the phase boundary requires a high sensitivity of the in situ method. Otherwise sampling is required, which can be disturbed by irreversible changes at the electrode surfaces.
2. The in situ experiments are time consuming with respect to the preparation of the experimental setup, the simultaneous data acquisition and the evaluation of all data.
3. For the determination of non-electrical properties of the electrochemical system special cells are required, the type and size of which are adjusted to the requirements of the spectroscopic method which might contradict the requirements of the electrochemical method in terms of electrode geometry, electrolyte composition, volume etc.
4. The selection of solvents, supporting electrolytes and the electrode materials is limited by the requirements of the spectroscopic method. It might be necessary to apply materials with less advantageous electrochemical properties.
5. The method applied can cause such an energy consumption of the spectroelectrochemical cell, which results in a change of the electrochemical reaction or the equilibrium at the electrode by structural changes.
6. The method applied might require the addition of such materials to the electrochemical system, which could change the electrode reaction.

Helmholtz compact double layer model (1879)

$$C_H = \frac{\varepsilon_r \varepsilon_0}{x_H}$$

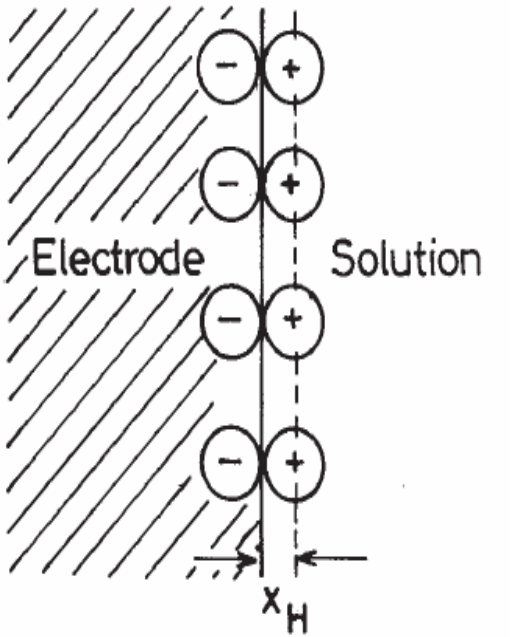

(a)

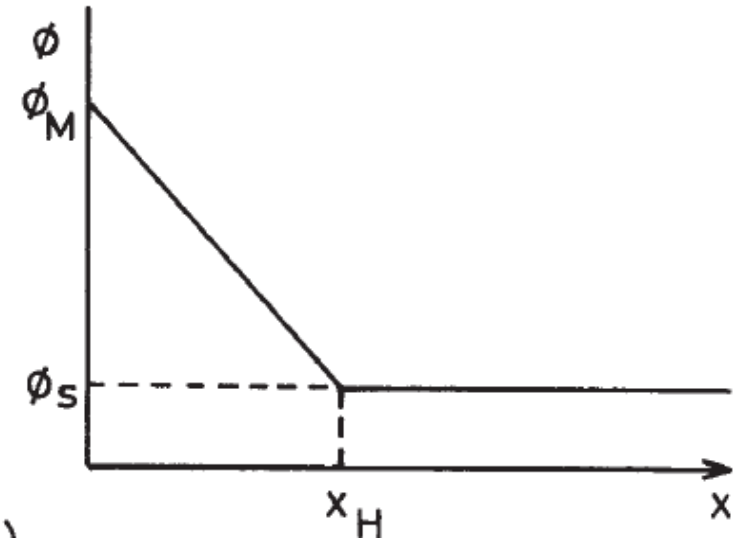

(b)

(a) Pictorial representation of Helmholz model of double layer with arrangement of point charges to give rise to a situation similar to parallel plate capacitor
(b) The variation of electrostatic potential ϕ as a function of distance x from the electrode

Gouy- Chapmann diffuse double layer model (1910-1913)

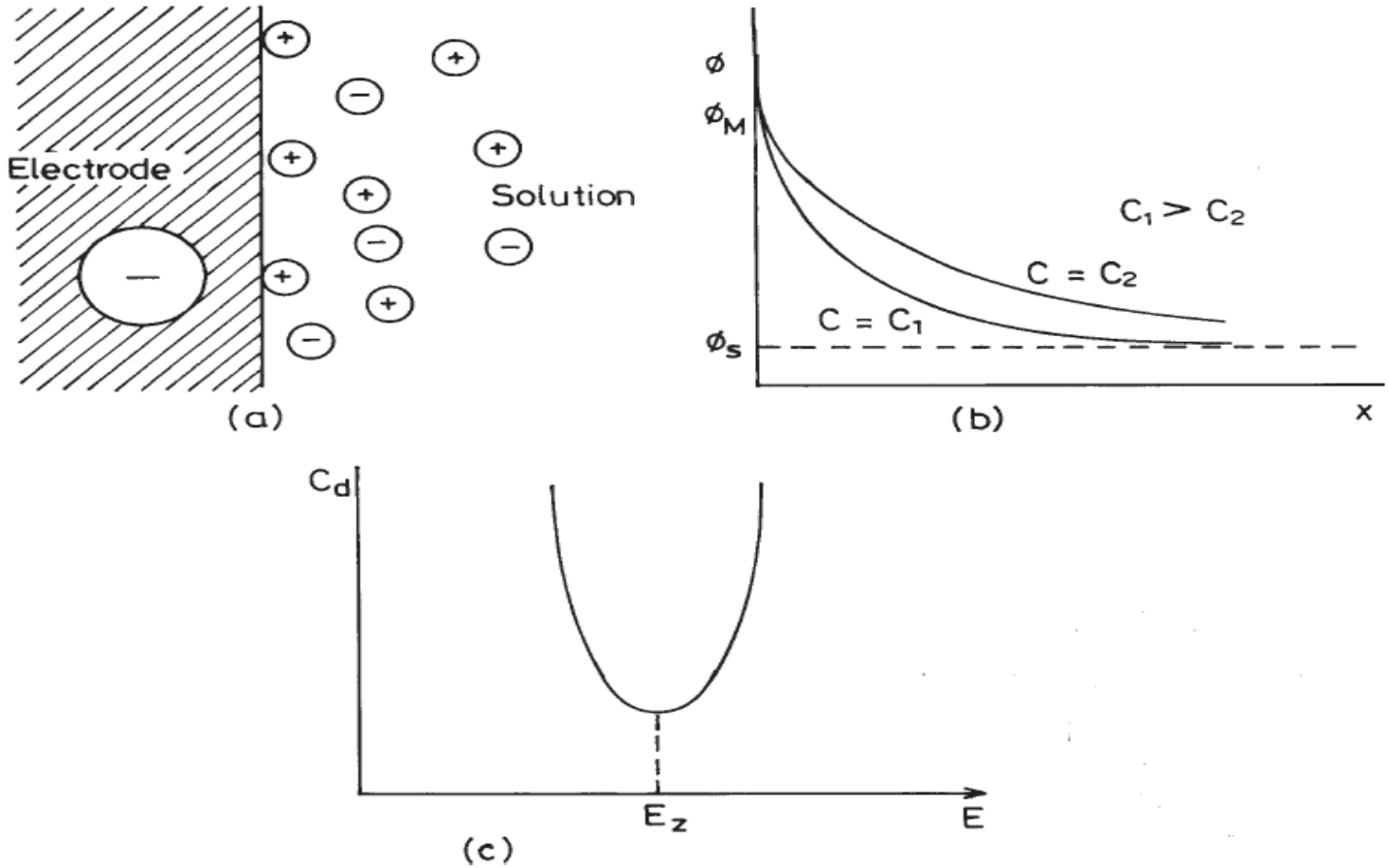

2.5 (a) Pictorial representation of ions in the diffuse double layer according to Gouy–Chapman model
(b) The variation of electrostatic potential ϕ as a function of distance x from the electrode. The variation of potential as a function of concentration of the ion is also shown in this figure
(c) Variation of C_d with potential, showing the minimum at the point of zero charge E_z

Stern compact diffuse layer model (1924)

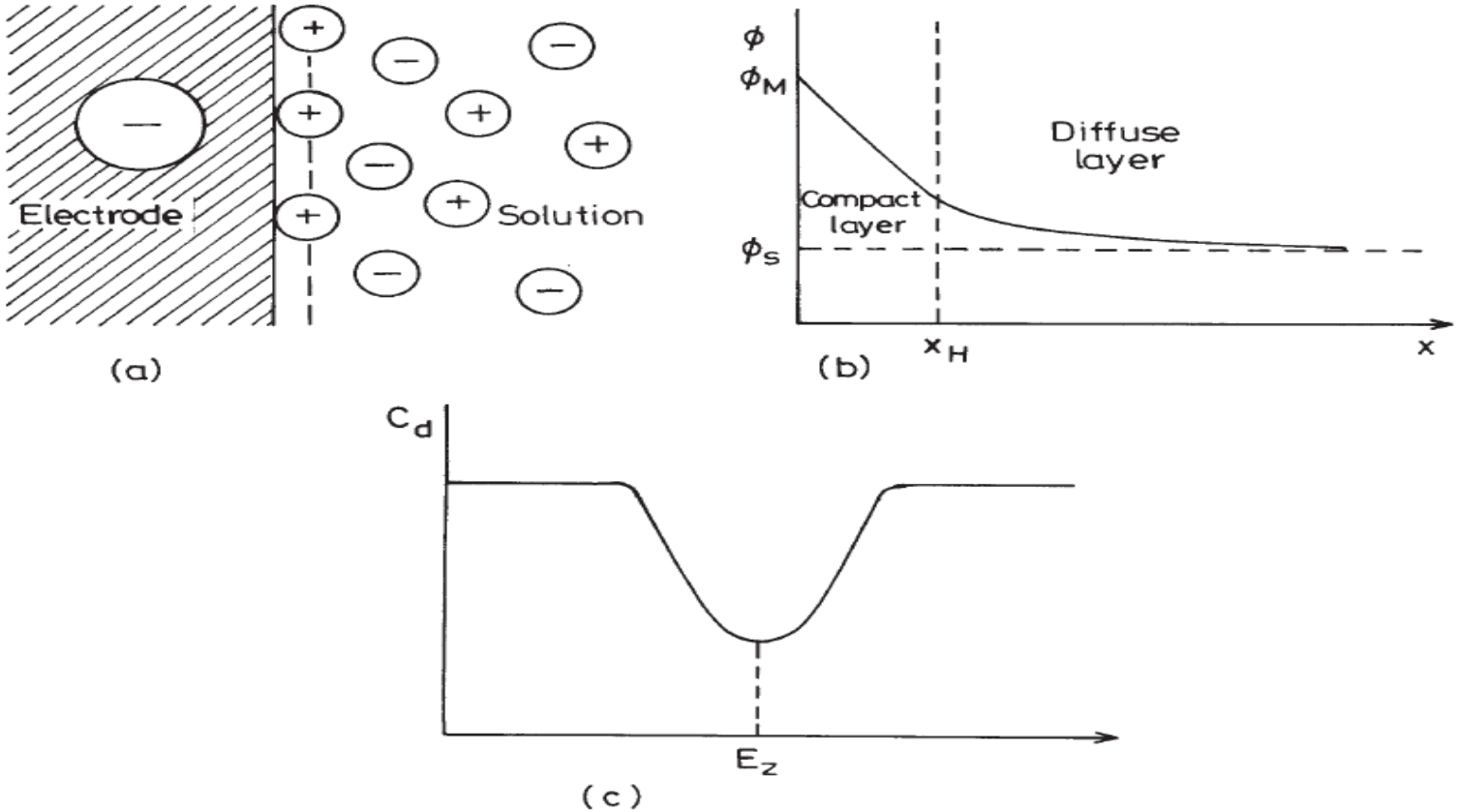

igure 2.6 Pictorial representation of Stern model of double layer (a) compact layer (similar to Helmholz double layer model) close to the electrode and a diffuse layer extending in the solution side (Guoy–Chapmann model); (b) and (c) the variation of potential ϕ and C_d with distance and potential respectively

Grahame triple layer model (1947)

Bockris, Devanathan and Muller model (1963)

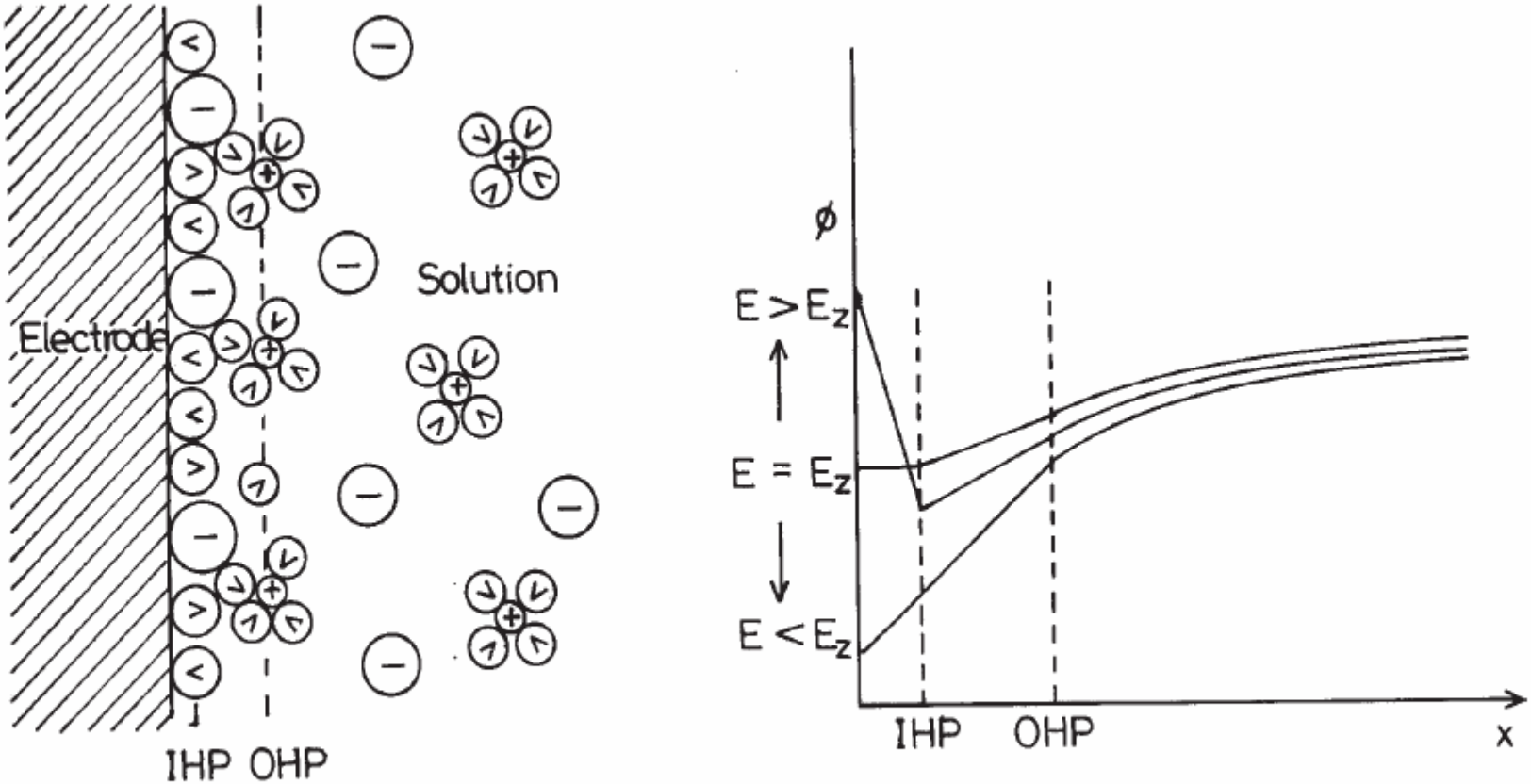

Figure 2.7 The double layer model of Bockris et al: (a) arrangement of ions and solvent molecules (^) represents a water molecule, and (b) the variation of electrostatic potential ϕ as a function of distance x from the electrode

2.2. The optical properties of a homogeneous phase

The optical properties of a homogeneous phase are described by a complex refractive index, $\hat{n}$ consisting of a refractive index, n, and an absorption index, k, and defined as

$$\hat{n} = n - \mathrm{i}\,k \tag{1}$$

according to the Nebraska convention (ref. 4), where i is defined as $\sqrt{-1}$. Instead of the complex refractive index, $\hat{n}$, the complex relative dielectric permittivity, $\hat{\varepsilon}_r$ can be used

$$\hat{\varepsilon}_r = \hat{n}^2 = \varepsilon_r' - \mathrm{i}\ \varepsilon_r'' \tag{2}$$

ε_r' and ε_r'' are related to the real and imaginary parts of $\hat{n}$ by the equations

$$\varepsilon_r' = n^2 - k^2 \tag{3}$$

$$\varepsilon_r'' = 2nk \tag{4}$$

provided that the relative magnetic permeability, μ_r, is unity.

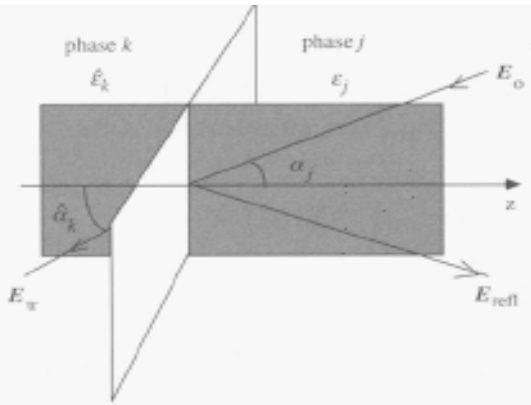

Fig. 1. Reflection and transmission of light at a smooth interface between two homogeneous phases *j* (transparent) and *k* (absorbing). E_0, E_{refl}, E_{tr}: incident, reflected, transmitted electromagnetic waves, respectively; $\varepsilon_j, \alpha_j, \hat{\varepsilon}_k, \hat{\alpha}_k$: relative dielectric permittivity and the angle of the light beam with the z-axis normal to the surface in phases *j* and *k*, respectively (in the absorbing phase *k* both ε and α are complex); the grey area is the plane of incidence, defined by E_0, E_{refl} and E_{tr}.

98 IUPAC, *Pure and Applied Chemistry* 70, 1395–1414

The electrode/electrolyte interphase consists of discrete or overlapping domains which may contribute to the spectroelectrochemical response. These domains would include

- the bulk of the electrode;
- the surface layer, influenced by the electric field: i) of the free electron gas (Thomas-Fermi layer); ii) of surface states; iii) of the bound electrons, if the electrode is a metal;
- the space charge layer and surface states, if the electrode is a semiconductor;
- the electrochemical double layer, consisting of an inner (Helmholtz) and a diffuse (Gouy-Chapman) layer;
- organic or ionic adsorbed species within the electrochemical double layer;
- multimolecular, inorganic and organic films;
- any films formed by reaction of the electrode with the environment (for example, oxide films);
- transport layers under hydrodynamic flow conditions, such as diffusion layers etc.;
- homogeneous reaction layers;
- migration or convection layers (if driving forces in addition to chemical potential gradients (diffusion) act on the transport processes);
- the bulk electrolyte.

REFLECTANCE EXPERIMENTS

UV/VIS Reflectance Spectroscopy

UV/VIS Differential Reflectance Spectroscopy

UV/VIS Electrochemically Modulated Reflectance Spectroscopy (or Electrolyte Electroreflectance Spectroscopy)

UV/VIS Wavelength Modulated Reflectance Spectroscopy

UV/VIS Laser Modulated Reflectance Spectroscopy

UV/VIS Attenuated Total Reflectance Spectroscopy (or Internal Reflectance Spectrosco

UV/VIS Surface Plasmon Spectroscopy

Infrared Reflectance Spectroscopy

Electrochemically Modulated Infrared Reflectance Spectroscopy

Differential Fourier Transform Infrared Reflectance Spectroscopy

Polarization Modulated Fourier Transform Infrared Reflectance Spectroscopy.

Multiple Internal Reflection Fourier Transform Infrared Reflectance Spectroscopy

METHODS BASED ON THE POLARIZATION OF LIGHT

Ellipsometry

Circular and Linear Dichroism

METHODS BASED ON SCATTERED LIGHT

Light Scattering from Non-flat Surfaces

Surface Raman Spectroscopy

Surface Enhanced Raman Spectroscopy

Nonlinear Optical Techniques

X-RAY AND γ-RAY TECHNIQUES

X-ray Diffraction

X-ray Reflection and Diffraction at Grazing Incidence

X-ray Standing Wave Fluorescence

EXAFS and Related Techniques

Mößbauer Spectroscopy

MAGNETIC RESONANCE METHODS, MICROWAVE SPECTROSCOPY

Electron Paramagnetic Resonance (EPR, ESR)

Microwave Absorption

Nuclear Magnetic Resonance (NMR) Spectroscopy

PHOTOCURRENT AND PHOTOPOTENTIAL SPECTROSCOPIES

PHOTOTHERMAL METHODS

Photoacoustic Spectroscopy (PAS)

Photothermal Probe Beam Deflection Spectroscopy

Probe Beam Deflectometry

LIGHT EMISSION METHODS

Electrochemical Luminescence

Electroluminescence of Semiconductors

Optically Transparent Electrodes

- A thick metal on a transparent substrate. Thickness must not exceed 100 nm for the film to remain transparent, and this can result in high electrical resistance
- A glass place with a thin film of optically transparent, conducting material,eg indium doped tin oxide (ITO)
- A gold minigrid between transparent substrates
- A thicker free standing metal mesh

UV/VIS Differential Reflectance Spectroscopy

The scheme of reflectance measurements is shown in Fig. 1. The intensity of the reflected beam is measured as a function of potential, and division by the intensity of the incident beam gives the reflectance, $\rho(E) = I_{\text{refl}}(E) / I_0$. The reflectance is measured at two potentials, a reference potential, ideally one at which the surface is film-free, and a potential at which a surface film (for example, an oxide or metal film) is formed. The normalized differential reflectance, $\Delta\rho(E) / \rho(E)$, is plotted versus potential or wavelength (ref. 22).

Differential reflectance spectroscopy is useful for obtaining absorption spectra of molecular films as a function of the redox state of the film, which depends on the electrode potential. Dye films with high enough absorption coefficients can be studied down to less than monolayer thickness.

Since the signal-to-noise ratio increases with the square root of the number of spectra accumulated, an ingenious rapid scanning spectrometer was developed (ref. 23), but it has been long superseded by photodiode or CCD arrays (optical multichannel analyzers (OMAs)), with which a whole spectrum can be collected in a few milliseconds. Data presentation should include the number of scans integrated and the integration time.

Comments: This method is suitable for investigation of multilayer films of oxides or metals, or monolayers of strongly absorbing molecules, atoms or ions. The method is also preferred for investigations at surfaces of single crystals. Sensitivity: $\Delta\rho / \rho < 10^{-4}$.

Measurement Modes

a) absorptance, α as a function of potential at a constant wavelength, $\alpha = f(U)_{\lambda}$ (absorptogram).

b) absorptance, α, as a function of the wavelength, $\alpha = f(\lambda)_{U}$ at a constant potential. This is the absorption spectrum of the solution or surface film,

c) absorptance, α, as a function of time after a potential perturbation, usually a potential step, $\alpha = f(t)_{\lambda}$ (chronoabsorptometry) Alternatively, a potential scan is used (voltabsorptometry). The derivative of the signal with respect to time has the shape of a cyclic voltammogram* (ref. 15).

IR Spectro Electro Chemistry

❖ From SEC one can derive the combined benefits of the techniques of electrochemistry and spectroscopy

❖ The oxidation and reduction processes in a redox active compound can be studied electrochemical cell specially designed for SEC technique.

❖ The products of the redox transformation or subsequent chemical reactions are monitored in situ by spectroscopic techniques.

❖ Recently Infra-Red (IR) SEC is used to study transition metal complexes and clusters containing IR-active ligands such as CO, CN-, RNC, or NO.

❖ A variety of transition metal clusters and complexes with ligands such as CO, CN^-, RNC or NO coordinated to metal centres can be studied by IR SEC (spectro electro chemistry)

.

❖ Recent studies include analysis of synthetic analogues of the all-iron Hydrogenase active site, the iron molybdenum cofactor of the nitrogenase enzyme, iron-sulphur and iron-molybdenum-sulfur clusters and nickel carbonyl clusters

IR Spectro Electro Chemistry (SEC)

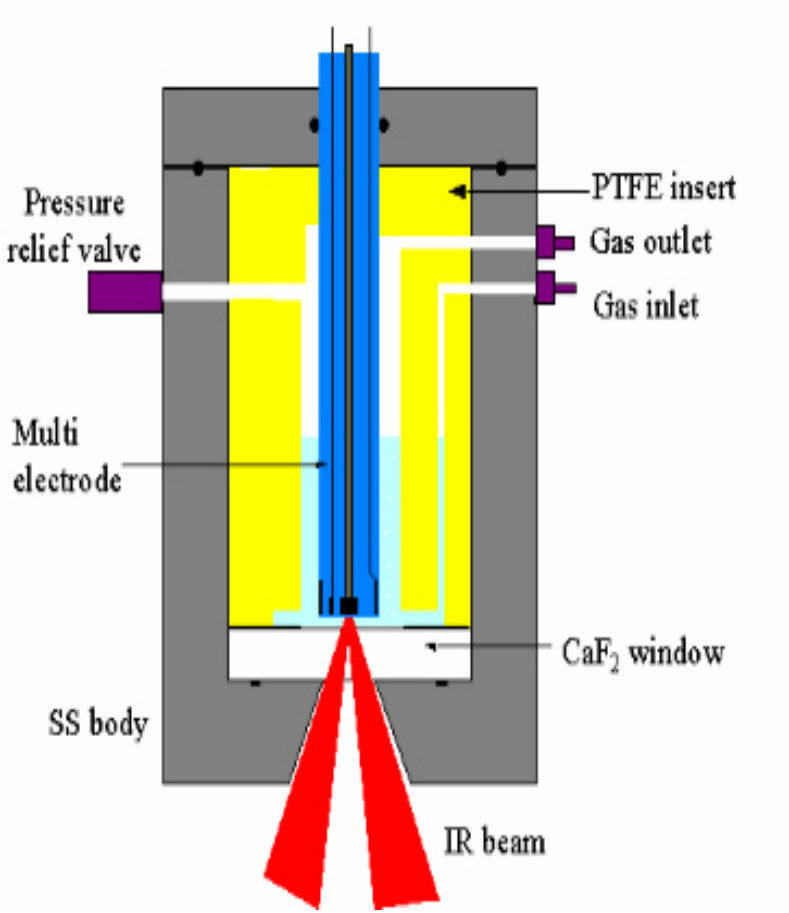

The fabrication of the Cell for IR SEC measurements

Fabrication of Cell for IR as well as UV-Vis Spectro Electro Chemical Experiments

- The spectroelectrochemical cell comprises of a three-electrode system into a central 'multi-electrode'

- Working electorde : A vitreous carbon, gold or platinum embedded at the centre of the KelF pin

- Reference electrode: A small silver is embedded beside the working electrode and Acts as a reference electrode

- Counter electrode: A platinum counter electrode is wrapped around the exterior of the KelF pin

- The multi-electrode is housed within a teflon insert in a stainless-steel body.

- A CaF_2 window forms the base of the cell and allows the IR beam to pass through a small volume of solution trapped between the electrode and the window.

- The beam is reflected off from the highly-polished surface of the central working electrode and back to the detector via a system of mirrors.

- Thus as the sample in the thin film between the electrode and the window is oxidised or reduced, IR spectra of the sample are recorded simultaneously.

What is Kel-F® and why is it used in the cell fabrication?

- Kel-F® is a homopolymer of poly chloro trifluoro ethylene
- Kel-F® has the lowest vapour transmission rate compared to any plastic
- Kel-F® is inert to chemicals and functions over a wide range of temperatures from – 400 to + 400 F
- Kel-F® has excellent electrical properties and can be machined to precise dimensions

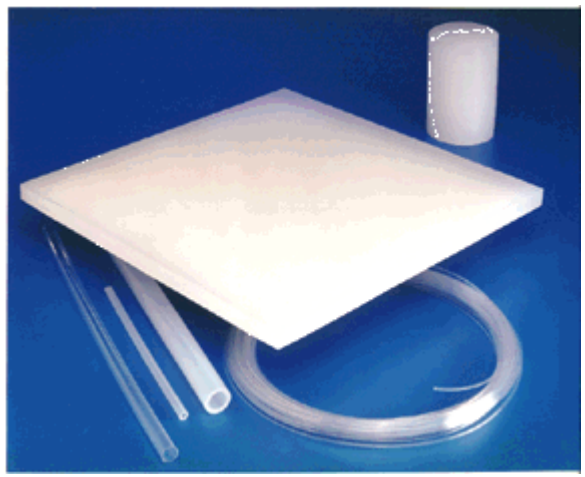

Kel-F

IR Spectro Electro Chemistry

❖ The Spectro Electro Chemical cell can be pressurised with a variety of gases up to pressures of 7 atm.

UV-Vis Spectro Electro Chemistry

❖ UV-vis SEC monitors changes in the UV or visible spectra as potentials are applied to the working electrode in the cell

❖ The UV-visible spectrophotometer shown below enables the use the same cell (as in the case of IR SEC to study changes in the UV or visible regions of the spectrum following oxidation or reduction of a sample

UV-Vis Spectro Electro Chemistry

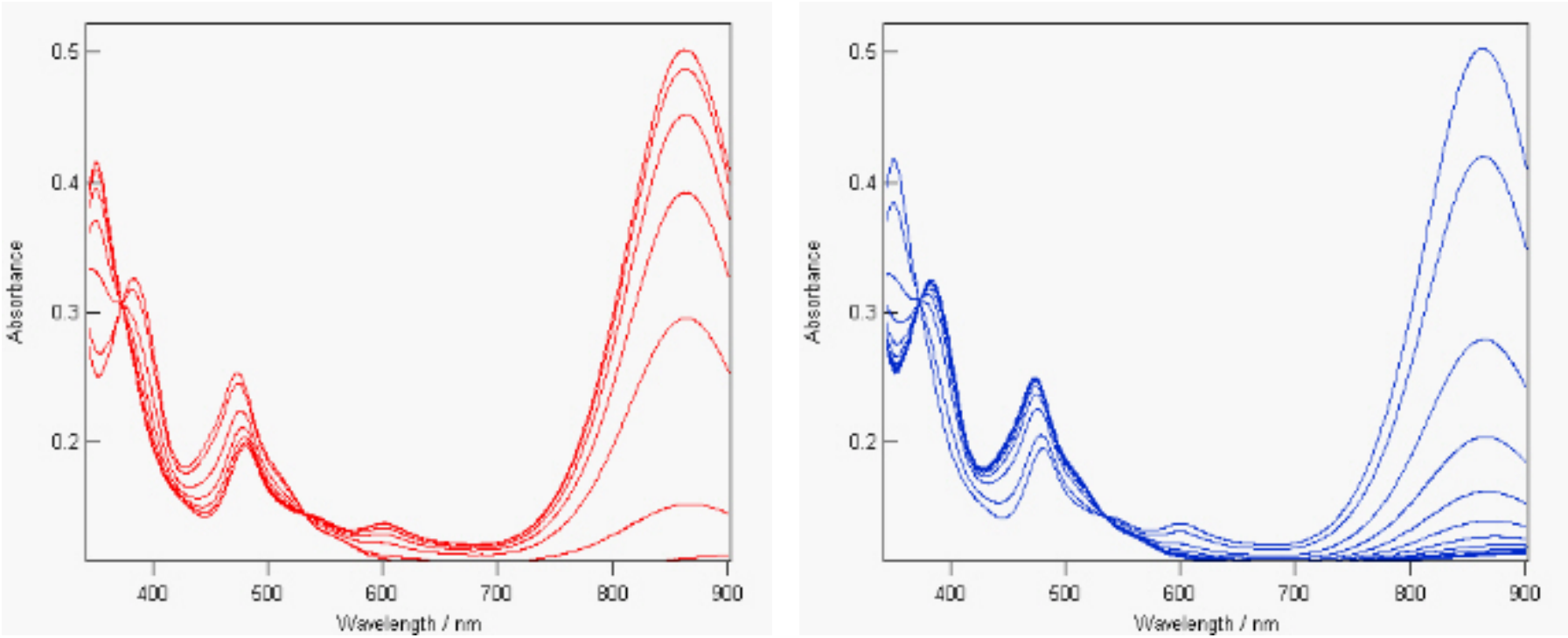

Spectra of of oxidation (red) and subsequent reduction (blue) of $[Ni^{II}(mnt)_2]$ complex

- Differential absorbance spectra showing the changes in the UV-vis region for the oxidation (red) and subsequent reduction (blue) of $[Ni^{II}(mnt)_2]$ (mnt – maleonitrile ditholate) complex are indicated above

- The complete set of spectra for each redox reaction were recorded in 5 seconds (oxidation) and 8 seconds (reduction)

Working Cell types

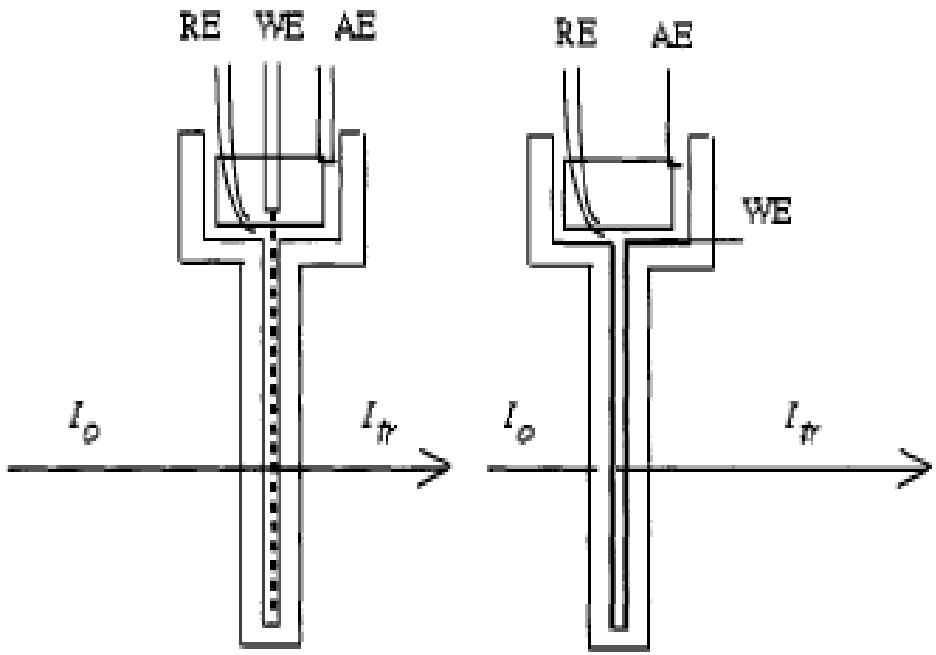

Fig. 2. Optically transparent electrochemical cells: a) minigrid as WE, b) evaporated cell wall as WE. I_0, I_{tr}, incident and transmitted intensity; WE, RE, and AE: working, reference and auxiliary electrode, respectively.

Investigations on thick films

Investigation of thick films: Special problems arise with thicker films.

- Multiple reflections at the film boundaries cause interference, the typical effect being a periodic increase and decrease of transmittance or absorptance at constant wavelength with growing thickness, or at constant thickness with changing wavelength. Although the first transmission extremum appears at a film thickness of $\lambda / 4n$ (n = refractive index of the film), already a film thickness less than $\lambda / 4n$ causes deviations from the Lambert-Beer law. Calculation of the optical constants of the film is recommended.
- A second problem is nonuniformity and roughness of the film. Several attempts have been made to take this problem into account (e.g. ref. 18).

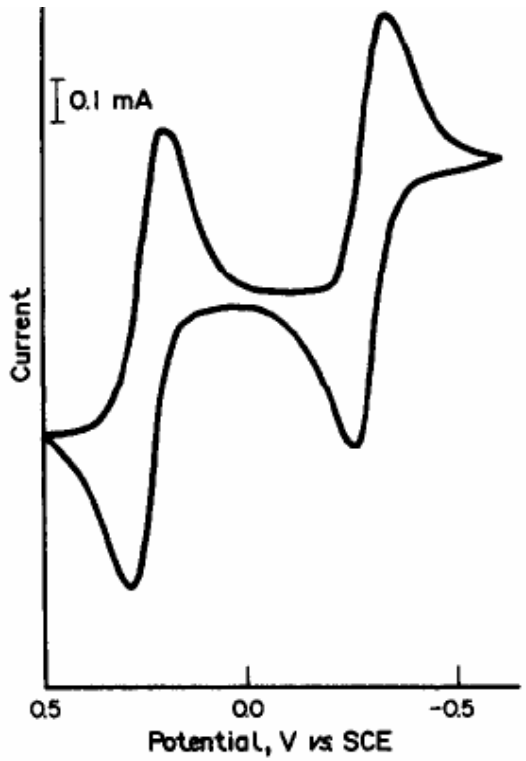

Fig. 4. Thin-layer cyclic voltamperogram of a solution of *5mM* TCNQ in acetonitrile (0.1*M* tetraethylammonium perchlorate supporting electrolyte) obtained in the cell described in Fig. 2. Potentials are *vs.* SCE, and the sweep rate was 5 mV/sec. Reproduced with permission from the American Chemical Society from Ref. 24.

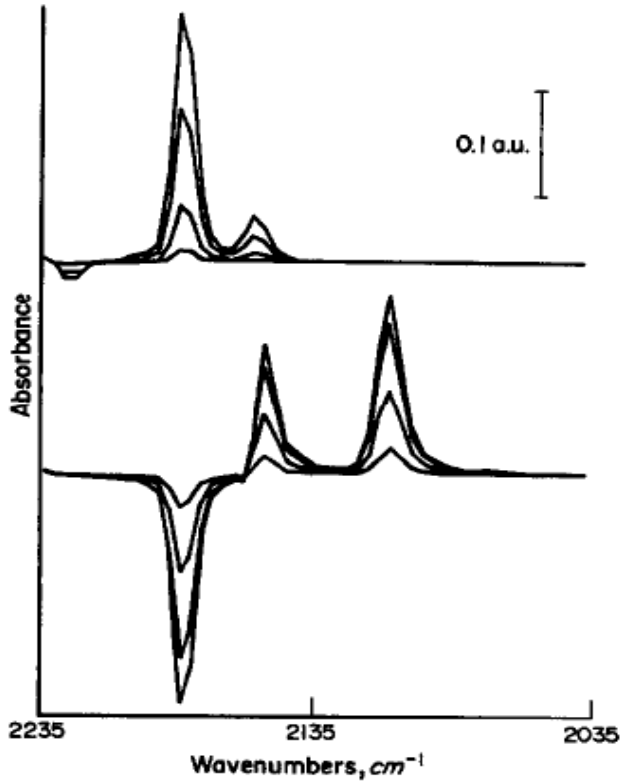

Fig. 5. Potential difference IR spectra obtained during reduction of TCNQ. Upper spectra (referenced to +0.5V): $E = 0.295$, 0.255, 0.210, and 0.130 V *vs.* SCE. Lower spectra (referenced to −0.15 V): $E = -0.250$, −0.315, −0.350, −0.400, −0.450 V. Reproduced with permission from the American Chemical Society from Ref. 24.

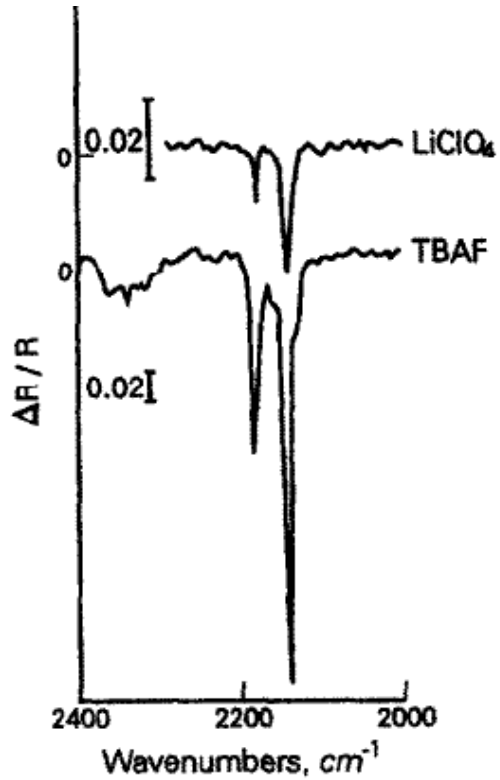

Fig. 6. Potential differential spectra in the C–N stretching region for the reduction of TCNE to TCNE at a Pt mirror electrode. Spectra were obtained with an external reflection cell similar to the cell described in Fig. 1. Solutions consisted of *5mM* TCNE in CH_3CN with either 0.1*M* $LiClO_4$ (top spectrum) or 0.1*M* TBAF (bottom spectrum) as background electrolyte. The potential was modulated from +0.5 V to −0.5 V *vs.* Ag/0.01*M* Ag^+ reference. Reprinted with permission from Elsevier Science Publishers from Ref. 40.

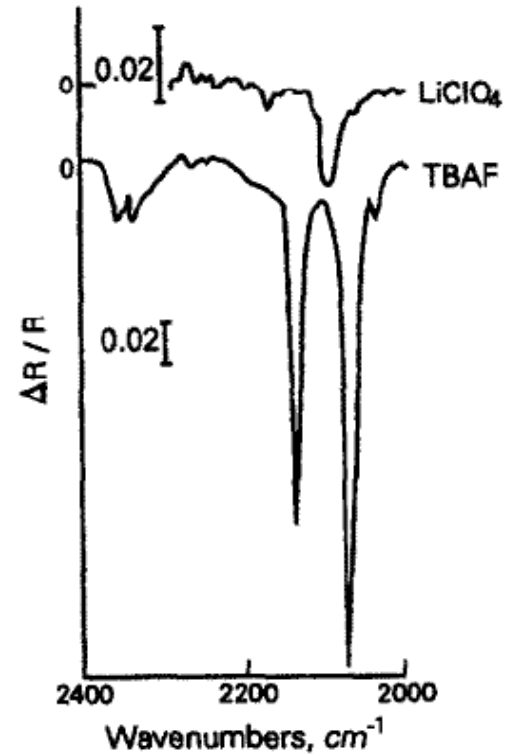

Fig. 7. PDIRS results (obtained in the C-N stretchi region) for the reduction of TCNE to $TCNE^-$ at I solution conditions and reference electrode are the same in Fig. 6. Top spectrum: 0.1*M* $LiClO_4$ as supporting electr lyte; potential modulated from +0.5 to −1.2 V. Botto spectrum: 0.1*M* TBAF as supporting electrolyte; potenti modulated from +0.5 to −0.2 V. Reproduced with pe mission from Elsevier Science Publishers from Ref. 40.

NIR Spectro-electrochemistry

1 spectroelectrochemistry of

-inorganic or organometallic transition metal compounds (including molecules of biochemical importance)
-conjugated organic molecules (neutral and radical)
-intrinsically conducting polymers

2 investigation of electrochromic compounds

Multiple species

Table 1. C≡N stretching infrared frequencies for various hexacyanoferrate complexes[43]

Complex	Wavenumbers, cm^{-1}
$Fe(III)(CN)_6^{3-}$	2116
$K_nFe(II)(CN)_6^{(4-n)-}$	2040
$K_nHFe(II)(CN)_6^{(3-n)-}$	2054
$K_nH_2Fe(II)(CN)_6^{(2-n)-}$	2067
$K_nLi_mFe(II)(CN)_6^{(4-n-m)-}$	2040
$K_nMg_mFe(II)(CN)_6^{(4-n-2m)-}$	2038
$K_nLa_mFe(II)(CN)_6^{(4-n-3m)-}$	2064

Summary of spectro-electrochemical studies on nanocarbon

The spectroelectrochemistry of fullerenes is focused on electron spin resonance studies of the spin states of fullerenes and the absorption spectroscopy of different fullerene cage structures and their charged states. Especially the role of mono-anions and the reactivity of higher charged state in C_{60} and its derivatives have made in situ spectroelectrochemical studies helpful.

The optical spectroelectrochemistry of SWNTs is used to follow the doping-induced bleaching of optical transitions among Van Hove singularities, including also excitonic and doping-induced absorptions. The electrochemical process is reversible and fast at the conditions of voltammetry. The spectroelectrochemical data are qualitatively consistent with the results of Vis-NIR spectra of chemically n-/p-doped structures, but the rate and reversibility of doping can conveniently be monitored only by spectroelectrochemistry.

The spectroelectrochemistry of SWNTs is dominated by resonance Raman spectroscopy. The Raman spectra are influenced both by the double-layer charging and by Faradaic processes. The radial breathing mode (RBM) is particularly suitable for investigations of tube-specific effects. The electrochemical charging of tubes with defined (*n, m*) chiralities provides inputs for the discussion of resonance Raman scattering, both in semiconducting and metallic SWNTs, but the correct interpretation of Raman spectroelectrochemistry in terms of excitonic effects still requires fundamental studies. The frequency and shape of the G-band are suitable for investigations of doping-induced changes of the C—C bond length, Fano broadening and other effects like Peierls-like transition in metallic SWNT. The G′-mode is more sensitive to electrochemical doping than the G-mode, but also strongly *k*-vector dependent. Implementation of the double resonance concept for the D and G′-modes might bring further inputs to spectroelectrochemistry of SWNTs.

What is the out come in nanocarbons research

- It is a useful tool in detailed description of doped states in nano carbons
- It differentiates different ways of doping
- It pushes the theoretical analysis of spectroscopic behaviour forward

Spectro-electrochemical Studies on Nano carbons

Spectroelectrochemistry of carbon nanostructures

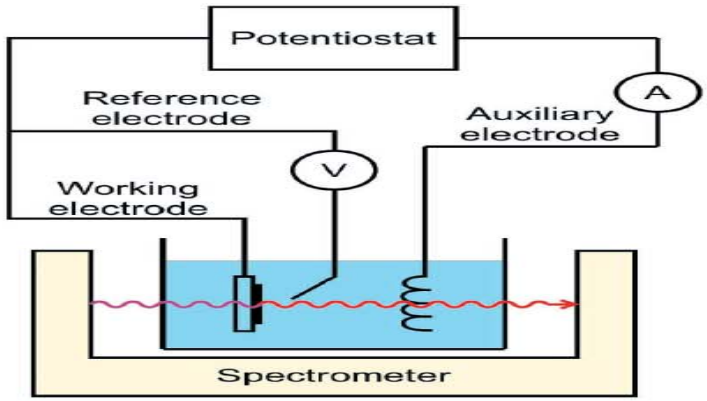

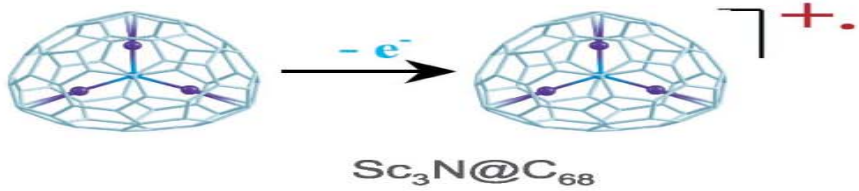

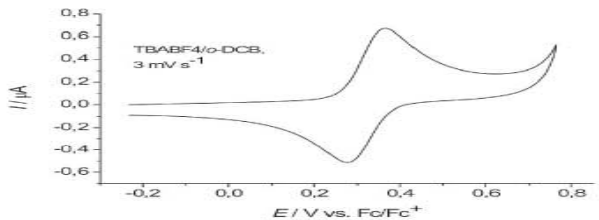

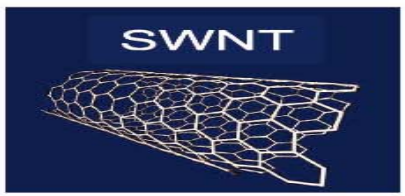

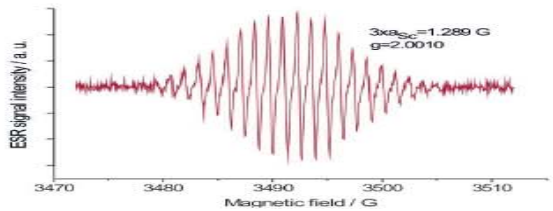

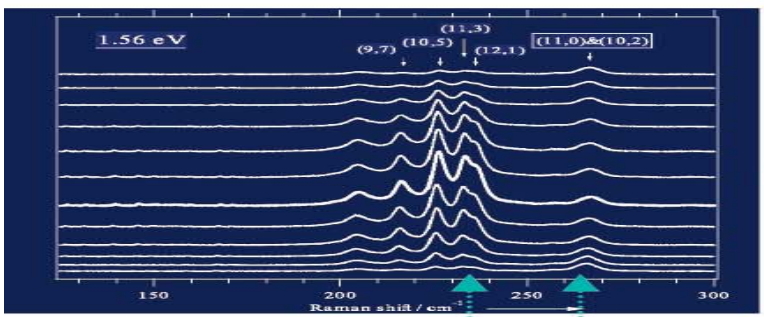

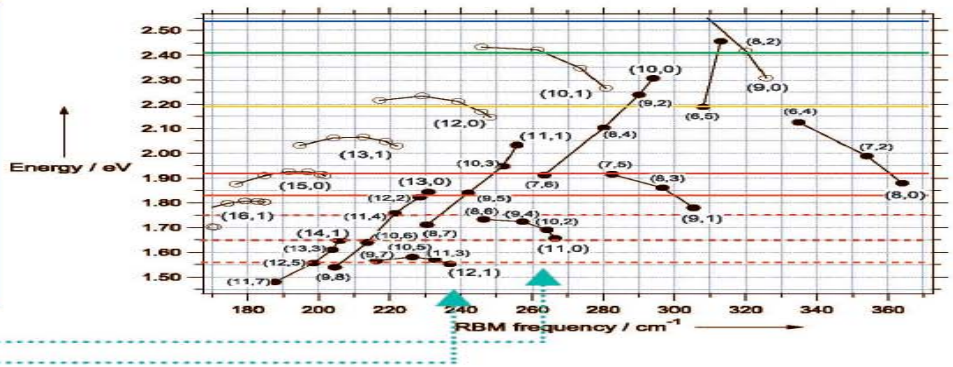

Spectro-electrochemistry of Self Assembled Monolayers of Biphenyl Ethynyl Thiols on Gold Electrodes

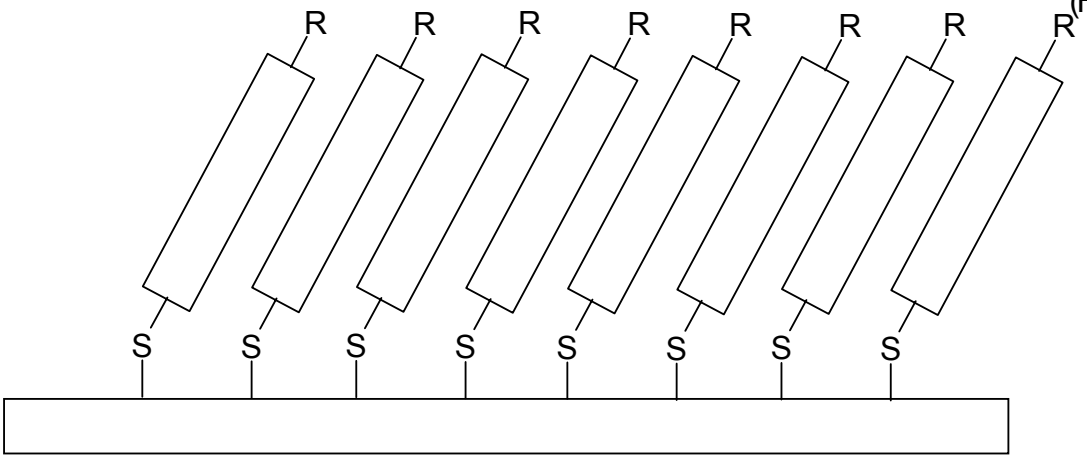

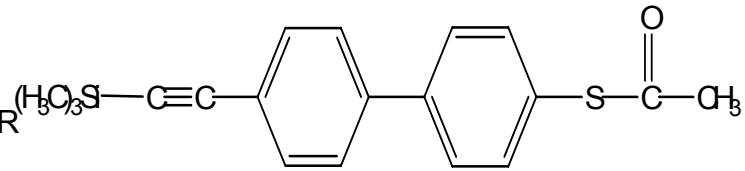

1

4-Trimethylsilylethinyl-4'-thiomethylester-1,1'-biphenyl

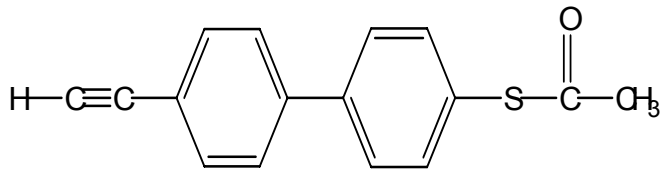

2

4-Ethinyl-4'-thiomethylester-1,1'-biphenyl

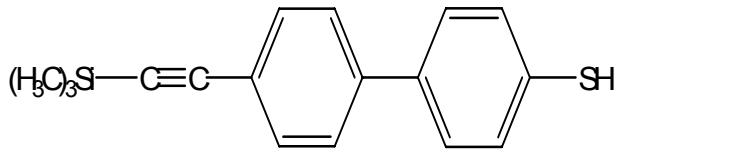

3

4-Trimethylsilylethinyl-1,1'-biphenyl-4'-thiol

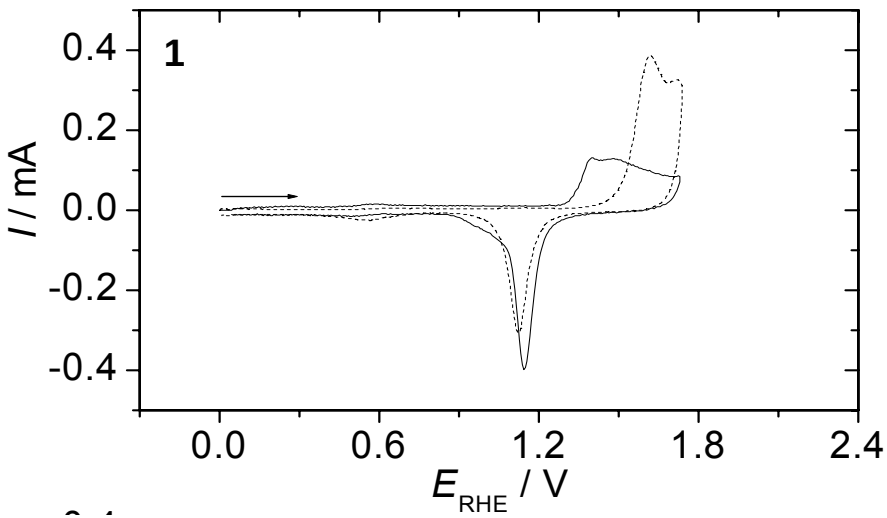

#	remaining free surface
1	73 %
2	66 %
3	37 %

SAM studies by Spectro- electrochemistry

	R_{CT} / Ω	C_{DL} / μF	*l* / nm of RS^-
Au	330	10.0	-
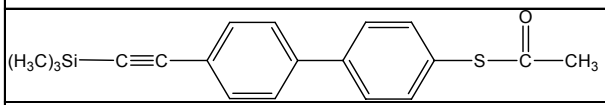 (**1**)/Au	2712	1.99	1.503
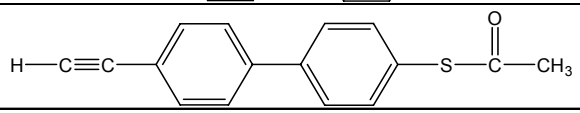 (**2**)/Au	2434	3.02	1.252
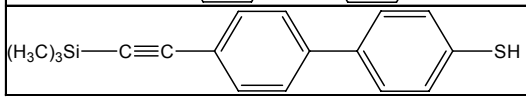 (**3**)/Au	2938	1.08	1.503

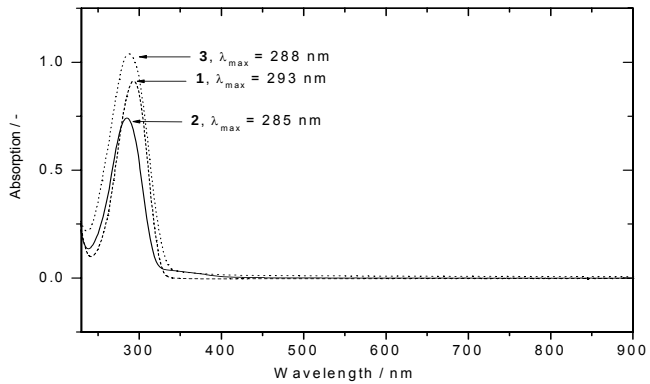

UV-Vis spectra of 10-5 mM of 1 in THF (a), 10-5 mM of 2 in THF (b) and 10-5 mM of 3 in THF (c), 5.0 mm cell, resolution 0.1 nm

0.01 **M** $(NH_4)_2Fe(SO_4)_2$/0.01 **M** $(NH_4)Fe(SO_4)_2$ in 1 **M** $HClO_4$

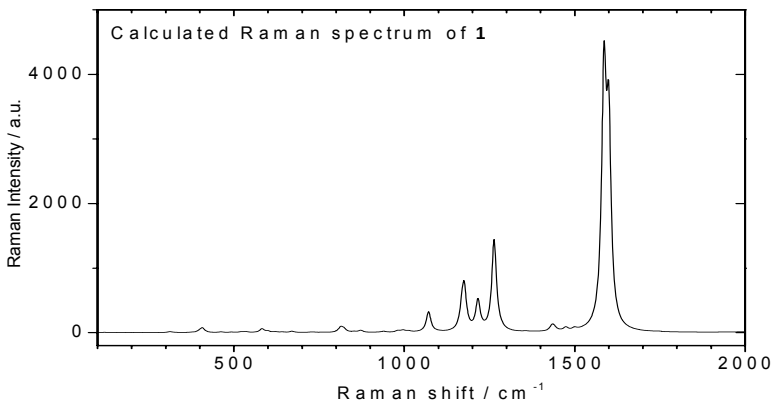

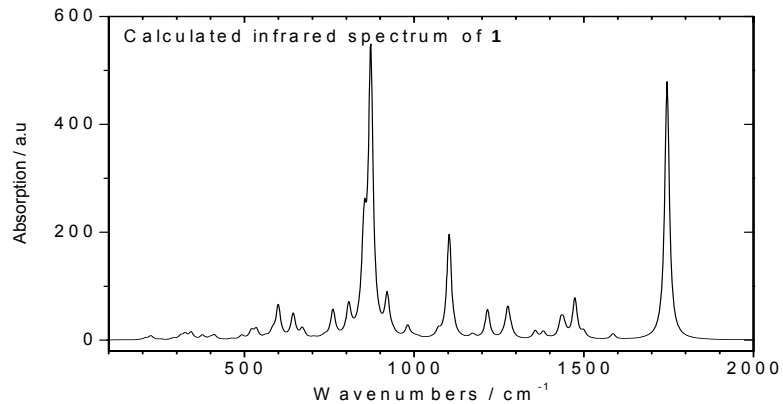

SAM studies by Spectro- electrochemistry

3

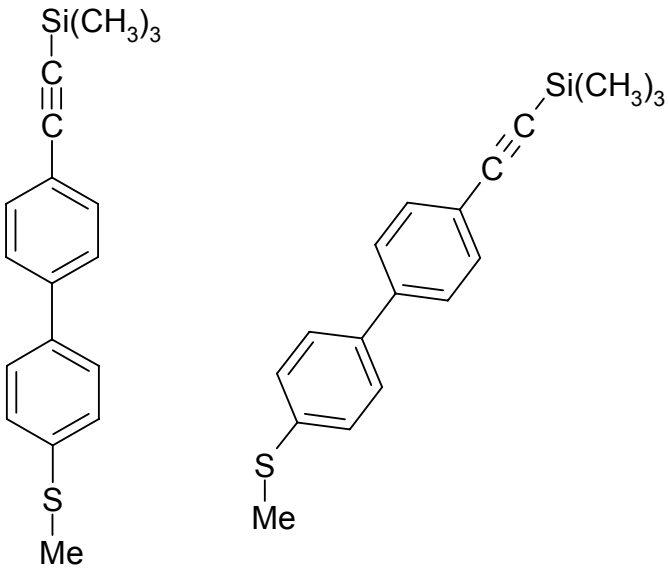

SAMs are formed

different compactness/thickness

Some are tilted with respect to surface normal

Various strengths of Au-S-interaction

Assignment of vibrational modes of **1** in solid form and the SER-spectra of a gold electrode coated with a monolayer of **1** in a solution of 1.0 **M** $HClO_4$ at various electrode potentials.

Assignment	Wilson mode #	IR	NRAS	SERS in 1.0 **M** $HClO_4$				
				E_{RHE}= 100 mV	E_{RHE}= 300 mV	E_{RHE}= 500 mV	E_{RHE}= 700 mV	E_{RHE}= 800 mV
n.a.	-	-	-	-	-	-	-	-
n.a.	-	-	-	-	-	-	184	187
$\nu_{Au?S}$	-	-	-	249	238	244	244	252
δ_{CH}	15	-	246	-	-	-	-	-
γ_{CH}	10b	-	325	-	-	-	-	-
γ_{ring}	16a	-	420	407	413	412	410	412
δ_{CH}	9b	450	-	465	468	473	474	476
n.a.	-	503	-	-	-	-	-	-
γ_{ring}	16b	538	-	-	-	-	-	-
n.a.		565	-	-	-	-	-	-
δ_{ring}	6b	613	-	-	-	-	-	-
ν_{CS}	-	632	633	622vw	622	621	621	628
n.a.	-	661	-	662	663	661	662	661
n.a.	-	699	-	-	-	-	-	-
δ_{ring}	12	-	745	-	-	-	-	-
$\beta_{as, methyl}$	-	759	762	-	-	-	-	-
γ_{CH}	10a	815	-	830	825	822	820	-
	17b	846	836	-	-	-	-	-
$\beta_{as, methyl}$	-	856	-	-	-	-	-	-
	-	-	874	-	-	-	-	-
γ_{CH}	17a	952	-	940	940	940	840	940
n.a.	-	1002	-	-	-	-	-	-
δ_{CH}	18a	-	1026	1019	1020	1020	1019	1019
	18b	1091	1106	1087	1086	1086	1084	1082
	9a	1190	1187	-	-	-	-	-
n.a.	-	-	1200	1195	1199	1199	1198	1198
ν_{CH}	7a	1250	1240	-	-	-	-	-
	13	-	1291	1289	1289	1290	1291	1290
δ_{CH}	3	1307	-	-	-	-	-	-
methyl def.	-	1352	-	-	-	-	-	-
	-	1388		-	1377	1377	1377	-
ν_{ring}	19b	1410	-	-	1399	1402	1401	-
	19a	1479	-	-	1484	1484	1483	1482
	8b	-	1604	1591	1592	1591	1591	1590
	8a	-	1612	1608	1608	1608	1608	1608
ν_{CO}	-	1707	-	-	-	-	-	-

v: stretch mode; def.: deformation mode; δ: in-plane deformation mode; γ: out-of-plane deformation mode; β_{as}: rocking mode.

Electrochemical and *in situ* spectroelectrochemical studies of gold nanoparticles immobilized Nafion matrix modified electrode

T SELVARAJU, S SIVAGAMI, S THANGAVEL and R RAMARAJ*

Abstract. Electrochemical and ***in situ*** spectroelectrochemical behaviours of phenosafranine (PS^+) were studied at the gold nanoparticles (Au_{Nps}) immobilized Nafion (Nf) film coated glassy carbon (GC) and indium tin oxide (ITO) electrodes. Cyclic voltammetric studies showed that the PS^+ molecules strongly interact with the Au_{Nps} immobilized in the Nf matrix through the electrostatic interaction. The presence of Au_{Nps} in the Nf film improved the electrochemical characteristics of the incorporated dye molecules. The emission spectra of $Nf–Au_{Nps}–PS^+$ films showed that the incorporated PS^+ was quenched by Au_{Nps} and it could be explained based on the electronic interaction between the Au_{Nps} and PS^+ molecules. The ***in situ*** spectroelectrochemical study showed an improved electrochemical characteristic of the incorporated PS^+ molecules at the $ITO/Nf–Au_{Nps}$ electrode when compared to the ITO/Nf electrode.

Bull. Mater. Sci., Vol. 31, No. 3, June 2008, pp. 487–494.

Spectroelectrochemical Sensing Based on Multimode Selectivity Simultaneously Achievable in a Single Device. 2. Demonstration of Selectivity in the Presence of Direct Interferences

Three modes of selectivity based on charge-selective partitioning, electrolysis potential, and spectral absorption wavelength were demonstrated simultaneously in a new type of spectroelectrochemical sensor. Operation and performance of the three modes of selectivity for detection of analytes in the presence of direct interferences were investigated using binary mixture systems. These binary mixtures consisted of $Fe(CN)_6^{3-}$ and $Ru(bpy)_3^{2+}$ and of $Fe(CN)_6^{4-}$ and $Ru(CN)_6^{4-}$ in aqueous solutions. Results on the $Fe(CN)_6^{3-}/Ru(bpy)_3^{2+}$ binary mixture showed that an anion-exchange coating consisting of PDMDAAC-SiO_2 [where PDMDAAC is poly(dimethyldiallylammonium chloride)] and a cation-exchange coating consisting of Nafion-SiO_2 can trap and preconcentrate analytes with charge selection. At the same time, such coatings exclude interferences carrying the same type of charge as that of the exchange sites in the sensor coating. Using the $Fe(CN)_6^{4-}/Ru(CN)_6^{4-}$ binary mixture, the $Fe(CN)_6^{4-}$ component can be selectively detected by restricting the modulation potential cycled to a range specific to the redox-active $Fe(CN)_6^{4-}$ component and simultaneously monitoring the optical response at the overlapping wavelength of 420 nm. It was also shown that, when the wavelength for optical monitoring was chosen as 500 nm, which is specific to the $Ru(CN)_6^{4-}$ component, interference from the $Fe(CN)_6^{4-}$ component for spectroelectrochemical detection of $Ru(CN)_6^{4-}$ was significantly suppressed, even though the cyclic modulation potential encompassed the redox range for the $Fe(CN)_6^{4-}$ component.

Anal. Chem. **1997,** *69,* 4819−4827

Reaction of 9-phenyl-2,3,7-trihydroxy-6-fluorone (H_3L) with $[Ru(bipy)_2(H_2O)_2]^{2+}$ affords the complex $[\{Ru(bipy)_2\}_2(\mu\text{-}L)]^+$ (3^+) which was isolated as its hexafluorophosphate salt; in this complex a $\{Ru(bipy)_2\}^{2+}$ fragment is coordinated to each dioxolene-like terminus of the bridging ligand $[L]^{3-}$. Voltammetric experiments in MeCN show the presence of three reversible one-electron redox couples at -0.36, 0.00 and $+0.53$ V *vs.* ferrocene/ferrocenium, which means that the complex is part of a four-membered redox chain spanning the oxidation states 3^+ to 3^{4+}. A spectroelectrochemical study in MeCN at -30 °C reveals a complicated series of electronic spectra in the different oxidation states which include some intense transitions in the near-IR region of the spectrum. The spectra could be partly assigned with the assistance of ZINDO calculations, which show that extensive mixing between the metal-centred and bridging-ligand-centred orbitals occurs; metal-to-ligand charge-transfer, ligand-to-ligand charge-transfer and intra-ligand transitions, amongst others, could be identified.

New J. Chem., 2000, **24**, 501–504

Electrochemical and spectroelectrochemical studies of cobalt-Schiff (Co-SB) base complexes, Co(salen) [N-N'-bis(salicylaldehyde)-ethylenediimino cobalt(II)] and Co(salophen) [N-N'-bis(salicylaldehyde)-1,2-phenylenediimino cobalt(II)], have been carried out to test them as oxygen reduction catalysts. Both compounds were found to form an adduct with oxygen and exhibit catalytic activities for oxygen reduction. Comparison of spectra obtained from electrooxidized complexes with those from Co-SB complexes equilibrated with oxygen indicates that the latter are consistent with the postulated complex formed with oxygen occupying the coaxial ligand position, namely, Co(III)-SB·O_2^{-}. The catalysis of oxygen reduction is thus achieved by reducing Co(III) in the oxygen-Co-SB adduct, releasing the oxygen reduction product, *e.g.*, O_2^{-}, from the Co(II)-SB complex.

Abstract: Mechanisms of electron transfer of carbazole (CZ) and 9-ethylcarbazole (ECZ) were studied by electrochemistry and *in-situ* spectroelectrochemistry. The result indicated that the electrochemical reaction mechanism of ECZ was the same as that of CZ. Both of them undergo ECE process: the initial step is removal of one electron to generate very reactive cation radical, this species then proceeded by deprotonation-coupling reaction to form the corresponding dimer, which was oxidized continuously.

Figure 3 Thin layer CV of 2 mmol/L ECZ

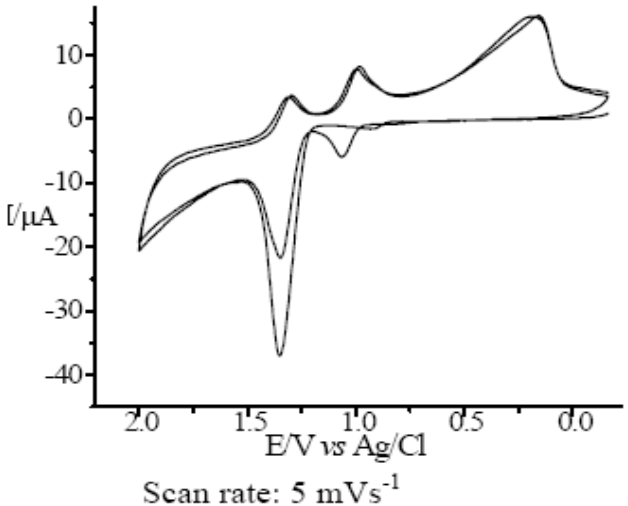

Figure 4 *In-situ* UV spectrum of 5 mmol/LECZ

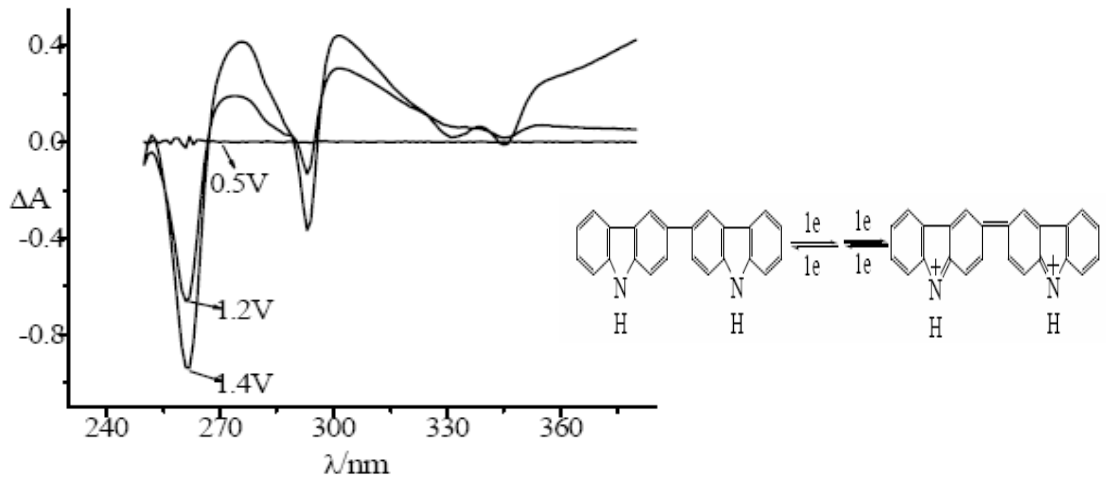

Chinese Chemical Letters Vol. 16, No. 12, pp 1621-1624, 2005
http://www.imm.ac.cn/journal/ccl.html

Bands(cm^{-1})	Assignment	Remarks
1631 (+)	(C=C)ring	1,2,4-substitute benzene ring ,proof of 3,3'-dicarbazyl
1560 (-)	(C=N)	increase or produce of C=N
1326 (+) 1306 (-)	σs (C-N)	influenced by chemical environments around, leading to red-shift
926 (+) 917 (-)	σ_{as} (C-N)	influenced by chemical environments around, leading to red-shift

An electrochemical and in-situ Raman spectroelectrochemical study of 1-methyl-3-propylimidazolium iodide ionic liquid electrolyte ($MPIm^+I_x^-$) in the absence ($x = 1$) and presence ($x = 3$) of iodine is presented. Cyclic voltammetric measurements in combination with a platinum disk microelectrode revealed a remarkable difference before and after addition of iodine to the ionic liquid, implying the electrochemical formation of polyiodide ions (I_5^-) at potentials more positive than +0.6 V in the presence of an equimolar amount of iodine. To verify this presumption, we performed in-situ Raman spectroelectrochemical measurements of $MPIm^+I^-$ and $MPIm^+I^- + I_2$ ionic liquids in a laboratory-made spectroelectrochemical cell, while stepwise changing the potential of the working platinum disk electrode. The results obtained were in good accordance with the above-mentioned postulate about the presence of polyiodide species (I_5^-), and can be conveniently employed in further investigations to elucidate of the Grotthus mechanism, associated with increasing conductivity as a

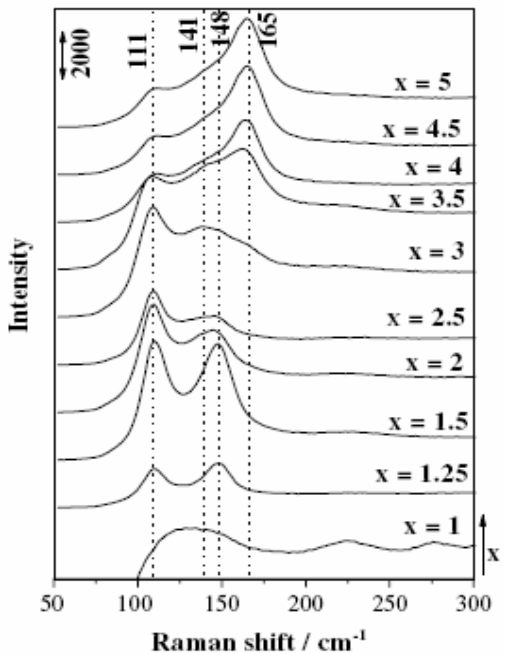

Fig. 2. Raman spectra of $MPIm^+I_x^-$ ($1 \leqslant x \leqslant 5$) obtained chemically by addition of iodine.

Electrochemistry Communications 9 (2007) 2062–2066

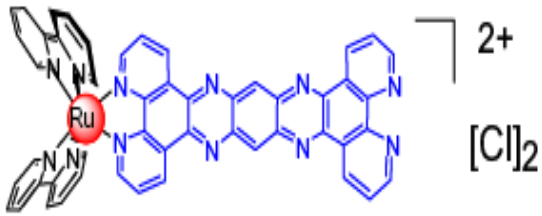

Fig. 1. Mononuclear ruthenium complex (1^{2+})

These data demonstrate that 1^{2+} is one of the few complexes capable of proton-coupled multi-electron transfers. This multi-electron storage capability is rooted in the overlapping of weak interacting bipyridine (bpy) and tetraazapentacene (tap) acceptor orbitals of the tatpp ligand. These orbitals seem to be essentially laminated on top of each other in a single fused aromatic system.

$$H_21 + 1^{2+} \rightarrow 2\,H1^{+}$$

Spectroelectrochemistry of $[(bpy)_2Ru(tatpp)]Cl_2$, a Photocatalyst for Hydrogen Generation

Reynaldo O. Lezna,[b] Norma R. de Tacconi,[a] and Frederick M. MacDonnell[a]
[a]Department of Chemistry and Biochemistry
The University of Texas at Arlington,
Arlington, TX 76019-0065

The reduction process of 1^{2+} was followed by UV-visible differential reflectance spectroelectrochemistry in a pH range from 10 to 2. At pH 10, the electrochemical reductions occur in two well separated potential windows (Fig. 2A), to generate the monoreduced 1^{+} (Fig. 2B, 850 nm), the doubly reduced 1^{0} (Fig. 2B, 706 nm) and protonated partner $H1^{+}$ (Fig. 2B, 580 nm) in the first potential window. The quadruple reduced 1^{2-} and related protonated H_21 species are formed in the second window.

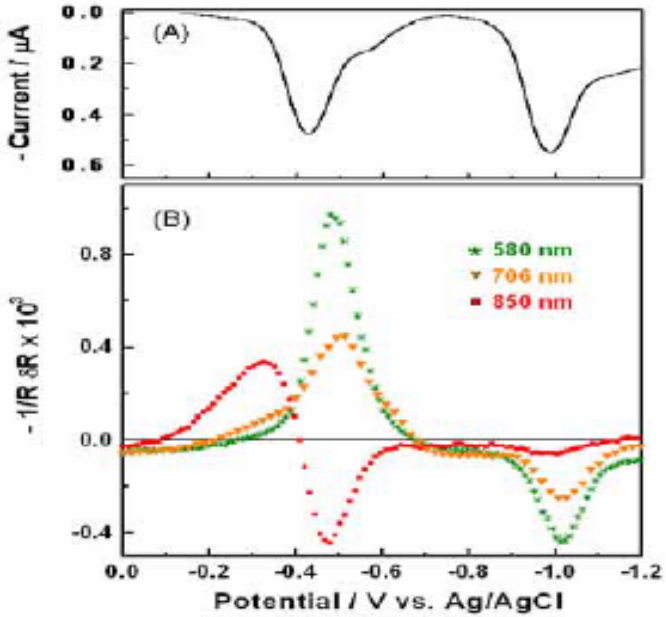

Fig. 2. (A) AC voltammogram for the electroreduction of 1^{2+} in water a pH 10.5 and **(B)** related differential reflectance (δV=0.04V, 11Hz) at three wavelengths to monitor 1^{+} (850 nm), 1^{0} (706 nm) and $H1^{+}$ (580 nm).

Spectro-electrochemistry on carbon nanomaterials

Two related spectro-electrochemical experiments were performed. In the first experiment voltages applied to a single walled carbon nanotube (SWCNT) thin film induced changes in the transmittance spectrum of the film. The changes are attributed to a voltage-modulated shift in the Fermi level of the nanotubes in the film. From this study the intrinsic doping level of the semiconducting carbon nanotubes was also determined. In the second experiment, an Indium Oxide thin film was subjected to varying voltages to change the film's free carrier electron density and thereby also modulate the film's transmittance. A spectroelectrochemical cell with high chemical resistance was designed for use in these experiments.

Spectroelectrochemical Study of Carbon Nanotube and Indium Oxide Thin Films

Jonathan Logan, Zhihong Chen, Partha Mitra, Jennifer Sippel, Andrew G. Rinzler

Department of Physics, University of Florida

Some of the References (only the selected ones)

- IUPAC document – Pure and Applied Chemistry, 70, 1395-1414 (1998).
- L.Kavan and L.Dunsch, ChemPhysChem,8,974-998(2007).
- K.Ashley, Talenta, 38,1209(1991)
- R.Holze, J Solid State Electrochemistry, 8,982-997(2004).
- And many more